A conceptual model of oceanic heat transport in a Snowball Earth scenario

Darin Comeau, Douglas A. Kurtze, Juan M. Restrepo
Center for Atmosphere Ocean Science, Courant Institute of Mathematical Sciences, New York University, New York, NY, USA

The authors thank both reviewers their time in providing for insightful comments and helpful critique on the manuscript.

Reviewer #1:

The authors use a low-order climate model to study the role of the ocean circulation and ocean heat transport for the initiation of hard Snowball Earth episodes (i.e., global sea- ice cover). Besides the investigation of the large-ice cap instability associated with a Snowball Earth, the authors further study the small-ice cap instability. To this end, they develop a simplified coupled atmosphere-ocean-sea-ice model in which the radiative effect of the atmosphere on the surface temperature is represented by a prescribed effective emissivity and the ocean is represented by four boxes with heat transport between them. The ice representation is the most complex part of the model as it includes flow of thick sea ice under its own weight (i.e., sea glaciers). The authors use the model to demonstrate that 1) ocean heat transport works against Snowball Earth initiation since a Snowball Earth results when they shut off the ocean circulation, 2) the heat exchange at the ocean-ice interface has a strong impact on the ice edge in this model, and 3) the Snowball ocean circulation can either be directed poleward or equatorward. I find the paper very interesting, well suited for Earth System Dynamics and a valuable contribution to the literature on Snowball Earth climate dynamics. I do have a couple of suggestions and comments though that I hope the authors will be able to address before publication.

Major Comments

1. *Atmospheric component of the model: there seems to be no representation of atmospheric heat transport, in contrast to the classic EBMs of Budyko and Sellers. Indeed, the Budyko and Sellers models only have multiple stable states because of atmospheric heat transport (Held and Suarez, 1974, Simple Albedo Feedback Models of the Ice Caps; Fig. 3). This seems worth pointing out because it implies that the bistability found in the model used here is different from the stability found in atmosphere-ice EBMs without ocean heat transport. It also makes me wonder to what extent the solutions would differ if a representation of atmospheric transport was included. I.e., would there be more equilibrium solutions, less, or the same? Answering this might require much work and might go beyond what is possible in the revision, but I would appreciate if the authors devoted some discussion to these points.*

Response: We certainly appreciate the importance of atmospheric heat transport in the global energy budget and climate system. Our modeling approach for the atmosphere was to simply provide a parameterization to express the net forcing of the atmosphere on the ocean and ice system, which was done through the radiative balance forcing in the effective emissivity parameter ϵ. Including atmospheric heat transport explicitly would require additional state variables of temperature at some atmospheric level, and then additional coupling parameterizations to the ocean and ice state variables of interest, which were the primary focus of the study. The Held & Suarez reference is certainly an appropriate one and has been added to the discussion of our model's bistability. The response of the ocean circulation in the bistability experiment shown in Figs 7 also responded with a hysteresis loop. Further discussion/clarity/disclosure on our modeling choice for the atmosphere has been added at the end of Section 2.2.

2. *The model is hemispherically symmetric and has no cross-equatorial ocean flow, but much*

of the ocean heat transport is achieved by the cross-equatorial AMOC in the present-day climate, with upwelling in the Southern Ocean and downwelling in the North Atlantic. So are comparisons between the Sv of the model?s ocean circulation and present-day observations really meaningful?

Response: Our hemispheric setup is similar to that of Griffies & Tziperman 1995, from which we get the reference hydraulic constant k. The comparison is just to state that our results are in a reasonable range, and we explore the model's sensitivity to this parameter governing the circulation strength in Section 4.

3. *Conductive heat flux at ocean-ice interface, Eqs. 3 and 4: the model includes heat conduction proportional to the temperature difference between the ice freezing temperature and the ocean temperature. But for salinities greater 24.7 the density maximum of sea water is at its freezing point and the formation of sea ice at the surface must therefore be preceded by convection due to stability reasons (e.g., Washington and Parkinson 2005; Voigt and Marotzke, Climate Dynamics 2010). So shouldn?t this term then not always be zero, since I expect salinities are above 24.7 psu. Apparently it is not, as is shown by the importance of that term, but it remains unclear to me why. Maybe for a partially ice covered box the ocean temperature will be above freezing temperature since otherwise the box was completely ice covered, but then it seems physically dubious to use the mean ocean temperature to parametrize the ocean-ice heat flux as this relies on the temperature of the ocean region where there is no sea ice, and hence no ocean-ice flux. How does this affect the result on the importance of the ocean-ice flux?*

Response: Convective instability at the ocean ice interface is a small scale process well below our model's resolution, and the role of the boundary layer parameter D is precisely to parameterize this unresolved process. As mentioned in the text, the ocean temperature used is a regularized temperature profile $T_{1,2}$ between the two ocean boxes to prevent an artificial temperature jump at the box boundary entering into the equation for ice melting / accumulation, and localize the bulk temperature information, precisely to minimize this effect of relying on ocean temperature in an ice-free area directly impacting ice production. In the end, this is still an approximation / modeling choice that was made to try to keep the model as simple and low-dimensional as possible, and is why we focus on the importance of this parameterization in our modeling results.

4. *Global-mean ice-accumulation rates: In equilibrium the global-mean ice- accumulation rate must be zero. In Fig. 2d, the global-mean of the red dashed line seems to be positive if looking at the blue axes, but now that I notice the red axes and that it might indeed be zero. So the blue and the red axes should have the same zero position. Related to this, the global-mean accumulation rate in a Snowball Earth state must be zero, but in Figs. 3d, 4d it is positive everywhere, and so the ice is still growing and the model is not yet in equilibrium. I suggest to run the model into true equilibrium. The final ice thickness will be set by the value of the geothermal heat flux.*

Response: This is a valid point and an oversight on our part, and new figures for the global glaciation experiment at true equilibrium are in the revised manuscript (Figures 3 - 6). The climate state in Figure 3 is changing much slower than its transition towards this state, though clearly not at equilibrium with net ice accumulation everywhere. Running the model further results in net melting in the tropics, as seen in revised Figures 3 & 4.

5. *It?s very interesting to see that the model can sustain a stable ice edge at 10-15 deg of the equator. This is similar to the Jormungand state (Abbot, Voigt, Koll, JGR 2011; Voigt and Abbot, Climate of the Past 2012) but must be for a different reason. In Abbot et al. and Voigt and Abbot, the stable low-latitude ice edge was made possible by the low albedo of snow-free sea ice and ocean transport was not important. Here, in contrast, the stability must be due to ocean transport, and a*

more detailed discussion of the physics that are involved in the stabilization of the ice edge by the ocean transport would be desirable.

Response: In short, the ice edge is stabilized by ice production/melting term (Eq. 10), is sufficiently negative as to overpower any ice advancing through advection. The role D, the parameterization of the ice - ocean energy exchange, plays a key role in determining the location of the ice margin, as seen in Figure 5.

6. *In the abstract the authors state that the presence of ocean heat transport works against Snowball initiation. But the impact seems to be non-monotonic according to Fig. 5c: I.e., an intermediate circulation strength (D=0.05) prevents global ice cover, but for both a lower and a higher value of D and thus a weaker and a stronger circulation the model falls into a Snowball.*

Response: Rather than the statement that ocean heat transport works against Snowball initiation, we clarify that an appropriate statement would be *poleward* heat transport works against Snowball initiation.

7. *The fact that the Snowball ocean can flow in both directions is interesting, and while it is mentioned in the text I feel that having a figure illustrating this should help. Maybe a more general schematic that describes the connection between ocean circulation and ice edge in the different climates?*

Response: With the revised simulations, in the studied parameter regimes we no longer see bistability of the ocean circulation direction.

Minor comments

1. The latitudinal coordinate θ has been changed from colatitude to latitude in the text, equations, and figures.
2. We respectfully disagree - integrating out longitude in the insolation equation (Eq. 7) results in a much messier looking expression that seems unnecessary.
3. Typo corrected.
4. Typo corrected.
5. The figures plot variables associated with the ice component, but there is no ice in the control climate referenced. The associated steady state ocean circulation and heat transport are summarized in Table 1.
6. The terms 'circulation constant' and 'hydraulic constant' were used interchangeably - this has been revised to only use 'hydraulic constant'.
7. The broken sentence has been edited out.
9. The symbols have been changed to triangles, pointing in the direction of the forcing change.

Reviewer #2:

I love a good box climate model, and the authors? approach to simplifying complex Snowball climate dynamics down to its fundamentals is admirable. However, the authors have made two serious errors in their analysis, one conceptual and one mathematical: 1) No model of global oceanic heat transport can neglect atmospheric heat transport: the latter is about six times as large as the former in the modern climate. 2) The authors? integrals calculating top-of-atmosphere heat fluxes and geothermal heat fluxes in equations 3-6 are missing a factor of 2 pi. In a surprising coincidence, these errors cancel each other out, leading to reasonable values for the model?s oceanic heat transport and temperature gradient. See the discussion below. I have two second-tier concerns: 3) I don?t

think the model has reached equilibrium, which calls into question the authors? results. 4) Like atmospheric heat transport, atmospheric water transport should not be ignored. Unfortunately, there?s not a simple fix which would allow the paper to be published with revisions. Solving problem #3 is easy. Fixing the math error in #2 is simple, but would result in a model climate which is wildly different from reality, because of the conceptual error #1. Fixing that would require major changes to the model, and a total reanalysis of the results. I rush to add that I really like the philosophy and goals of this paper, and when the authors have addressed the flaws I?ve outlined here, I would love to review the new manuscript. I discuss these problems in more detail below, along with additional minor comments.

Major Comments 1. *1) Neglect of atmospheric heat transport. For a given surface temperature, the net heating or cooling of each latitude is fixed by the top-of-atmosphere radiation balance (Trenberth and Caron 2001, Figure 1). Any imbalance in TOA radiation in a given latitude band must be compensated by net heat transport into or out of that band (TC01, Figure 2). This could be achieved by atmosphere or ocean, but in the present-day climate, only about 1/5 of this is carried by the ocean: the atmosphere does most of the work (TC01, Fig 7). The authors? ocean model is driven directly by TOA radiation balance integrated over the surface of their box, and the integrand is a good match to observations (TC01 Fig 1). The integral of TOA radiation over the tropical box should amount to 5 petawatts, as in observations, but unlike the real world, in their model all of this must be transported by the ocean: their ocean?s heat transport must be five times greater than reality. To achieve this, the model?s ocean circulation would need to be five times more vigorous, or the tropic/polar temperature difference about five times greater, than is observed. This would make the model?s base climate so divergent from reality that their Snowball experiments ? which depend crucially on meridional temperature gradient ? would be called into question. However, on Page 16, they note that the model produces quite reasonable ocean circulation and temperature gradients. How can this be? Their integral of TOA radiation is too small by a factor of 2 pi, which nicely cancels out the neglect of the atmosphere in the modern-day climate (Point 2 below). The atmospheric heat transport could be included in a box model. I would suggest the authors track surface air temperature separately from ocean temperature: determine it diagnostically by a balance between TOA radiation, atmospheric heat transport from one box to the other, and air-sea heat exchange:* $TOA = F_atmos + F_airsea$ *Let flux between atmospheric boxes, and exchange between air and sea be governed by the same sort of mixing dynamics used for the ocean boxes, with exchange constants tuned to match observations. Crucially, there is no time derivative in this equation, so the atmosphere temperatures can be solved algebraically given the temperature of the ocean boxes in each timestep. The oceans would be forced entirely by* F_airsea *in such a model, rather than the TOA fluxes: since these are weaker, the ocean circulation would be in line with observations. It?s all quite doable, but it?s a different paper than the one the authors have submitted. If they wish to go in this direction, I would be delighted to review the manuscript again in the future.*

Response: We certainly agree that atmospheric heat transport is crucial to the global climate system and energy budget. Our modeling approach was to incorporate the atmosphere as a forcing, rather than a coupled aspect of the model. The air-sea heat flux component is an important aspect of heat transport, but at coarse spatio-temporal scales it is important to understand the basic state of outcomes before adding these fluxes with their very strong dependence on local/resolved dynamics. We believe we are not asserting that the model is not transporting all of the planet's heat through the ocean, as is stated by the reviewer. The atmosphere is a forcing in our model through ϵ - heat transport within the atmosphere is not modeled, but is all wrapped up in ϵ - perhaps having different ϵs for each box (or even a pole-to-equator profile) could mock up varying atmospheric forcing by latitude, at the cost of introducing another parameter.

We believe we are not asserting that the model is not transporting all of the planet's heat through

the ocean, as is stated, and think this sentiment is key to the reviewer's discomfort with our lack of an explicit, dynamic atmosphere. The atmosphere is a forcing in our model through ϵ - heat transport within the atmosphere is not modeled, but is all wrapped up in ϵ - perhaps having different ϵs for each box (or even a pole-to-equator profile) could mock up varying atmospheric forcing by latitude, at the cost of introducing another parameter. The atmosphere may well transport six times as much heat - our approach is that the net effect of the atmosphere (including heat transport within the atmosphere) on the ocean / ice coupled system is through the radiative balance via ϵ. Further discussion/clarity/disclosure on our modeling choice for the atmosphere has been added at the end of Section 2.2.

We thank the reviewer for the useful Trenberth and Caron reference, particularly Figure 5 for reference ocean heat transport values.

2. *Missing factor in integrals. The integrals in equations 3-6 are intended to be integrals of a vertical flux (watts per square meter) over the surface area of the box, to give a total flux in watts. They are obtained by multiplying the flux at each colatitude by the area of a thin circular "ribbon" encircling the globe at that colatitude, and then adding up all such ribbons. The north-south height of the ribbon is* $dy = r_e * dtheta$*; its east-west length is the circumference of the globe at that colatitude,* $2 * pi * r_e * sin(theta)$*. The* $2 * pi$ *factor is missing from these equations. As a result, the authors? radiative forcing is 6.28 times weaker than it should be!*

Response: We thank the reviewer for pointing out this glaring missing factor. We have corrected our code and manuscript with the 2π integral factor, and have rerun all simulations to provide revised all results in the manuscript.

3. *Model not at equilibrium. I was alarmed by the statement on Page 18: that the ice thickness increases continuously in the fully glaciated model. Eventually, the ice should thicken enough that geothermal heat input to the ocean balances conductive heat loss through the ice shell. Goodman et al (2003) argue that this should happen at an ice shell thickness of 1200 meters, and in their model equilibrium is achieved only after 30,000 years. It?s possible the authors? model is not yet at equilbrium: they shows a thickness of just 300 m (and still thickening), achieved after a shorter run of 20,000 years. The authors? model may take even longer to reach equilibrium than Goodman (2003), because their ice boundary layer parameterization may limit the rate of heat transfer.*

Response: This is a valid point also raised by Reviewer #1. The climate state in Figure 3 is changing much slower than its transition towards this state, though clearly not at equilibrium with net ice accumulation everywhere. We have provided revised simulations with model for Snowball Earth in equilibrium after 500,000 years. The system changed very slowly after global glaciation was reached, gradually accumulating ice until a region of net melting formed in lower latitudes to balance polar ice production. Of course, in comparative runs with ocean circulation turned off, equilibrium could not be reached as geothermal heat flux had no contact with the ice layer, and ice does (slowly) continue to accumulate with no mechanism in place to allow for melting.

4. *Atmospheric moisture fluxes. Goodman (2006) finds that about 20% of the thickness of a sea glacier would be composed of ice derived from snowfall ("meteoric" rather than "marine" ice.) And that?s in a hard snowball climate where precipitation is measured in mm per year! In the partially-glaciated cases considered here, the thickening and flow of the ice sheet due to snowfall probably cannot be neglected. A box-model-style mixing parameterization between atmospheric boxes, with a Clausius-Claperyon dependence on temperature could probably be used here.*

Response: We were aiming for the simplest model that would capture ocean heat transport in Snowball Earth scenario, and the addition of atmospheric moisture flux would have increased complexity beyond the scope of the study. We certainly agree that precipitation minus evaporation

is missing from the model and would quantitatively affect the results, though we would expect the main results of our study regarding ice/ocean interaction through heat transfer and its affect on the global climate state to stand. Furthermore the lack of atmospheric moisture was mentioned at the end of the original manuscript as an area for future work.

Minor comments

1. The note and reference has been added to the text.
2. Typo corrected.
3. The variables related to box quantities have been relabeled from box number to ut, up, dp, dt for upper tropic (Box 1), upper polar (Box 2), deep polar (Box 3), and deep tropic (Box 4), respectively.
4. While recent observational basal melt rates under ice shelves are available (notably Rignot et al 2013 (Science), Depoorter et al 2013 (Nature), and Schodlok et al 2015 (JGR: Oceans), the authors are not aware of an observational ocean temperatures under ice shelves, though pursuing this with GCM simulation or reanalysis data to form an estimate of D would be valuable future work.
5. Typo corrected.
6. Correct, the insolation equation is (mistakenly) for $\theta =$ latitude as written. Per another reviewer's request, we have converted θ from latitude to colatitude everywhere.
7. With the code modifications addressed, we actually now see poleward circulation in the Snowball simulations, consistent with the reviewers comments.

Manuscript prepared for Earth Syst. Dynam.
with version 2014/09/16 7.15 Copernicus papers of the LaTeX class copernicus.cls.
Date: 29 August 2016

A conceptual model of oceanic heat transport in the Snowball Earth scenario

Darin Comeau[1], Douglas A. Kurtze[2], and Juan M. Restrepo[3]

[1]Center for Atmosphere Ocean Science, Courant Institute of Mathematical Sciences, New York University
[2]Department of Physics, Saint Joseph's University
[3]Department of Mathematics, College of Earth, Ocean, and Atmospheric Sciences, Oregon State University

Correspondence to: Darin Comeau (comeau@cims.nyu.edu)

Abstract. Geologic evidence suggests that the Earth may have been completely covered in ice in the distant past, a state known as Snowball Earth. This is still the subject of controversy, and has been the focus of modeling work from low dimensional models up to state of the art general circulation models. In our present global climate, the ocean plays a large role in redistributing heat from the equatorial regions to high latitudes, and as an important part of the global heat budget, its role in the initiation a Snowball Earth, and the subsequent climate, is of great interest. To better understand the role of oceanic heat transport in the initiation of Snowball Earth, and the resulting global ice covered climate state, the goal of this inquiry is two-fold: we wish to propose the least complex model that can capture the Snowball scenario as well as the present day climate with partial ice cover, and we want to determine the relative importance of oceanic heat transport. To do this, we develop a simple model, incorporating thermohaline dynamics from traditional box ocean models, a radiative balance from energy balance models, as well as the more contemporary 'sea glacier' model to account for viscous flow effects of extremely thick sea ice. The resulting model, consisting of dynamic ocean and ice components, is able to reproduce both Snowball Earth as well as present day conditions through reasonable changes in forcing parameters. We find that including or neglecting oceanic heat transport may lead to vastly different global climate states, and also that the parameterization of under ice heat transfer in the ice/ocean coupling, plays a key role in the resulting global climate state, demonstrating the regulatory effect of dynamic ocean heat transport. ~~Furthermore we find that the ocean circulation direction exhibits bistability in the Snowball Earth regime.~~

1 Introduction

It is well known that the albedo difference between sea water and sea ice leads to a crucial climatic feedback. In a warming climate, melting of high albedo sea ice exposes low albedo sea water, thus increasing the fraction of incoming solar radiation that is absorbed and thereby amplifying warming. Conversely, in a cooling climate the growth of sea ice increases the planetary albedo, which amplifies cooling. Classic energy balance models (EBM)s demonstrate how this well-known ice-albedo feedback can lead to multiple steady climate states (Budyko, 1969; Sellers, 1969). Given forcings which resemble present-day conditions, these models are bistable, with one possible steady state having a partial ice cover and another being completely ice free. With a sufficient reduction in the solar input or the greenhouse effect these energy balance models yield completely ice-covered steady states, reminiscent of the "Snowball Earth" episodes of the Neoproterozoic era.

The virtue of simple models, of course, is that they make it possible to explore ranges of relevant parameters easily. First order energy balances at climatic scales are overwhelmingly radiative. The first energy balance models were not intended to model meridional energy transport, and if included, it was incorporated as a diffusive process. Diffusion-dominated transport tends to mitigate the tendency for sea ice to grow in a cooling climate: formation of extra sea ice would increase the temperature contrast between the ice-covered high latitudes and the low latitudes, which in turn would increase the rate of heat transport to the high latitudes. This then slows the growth of the ice, and exports some of the excess cooling due to the ice-albedo feedback to lower latitudes.

While the small ice cap instability has been a common phenomenon in EBMs (Held and Suarez, 1974), this bistability has not been seen in more sophisticated general circulation models (GCMs) (Armour et al., 2011). In a recent study, Wagner and Eisenman (2015) showed the bistability does not appear when an EBM was combined with a single column model for ice thermodynamics, suggesting sufficient complexity, including a seasonal cycle and diffusive heat transport, eliminate this bifurcation. While the small ice cap instability is not the primary focus of this study, we will use our model to investigate this small ice cap bifurcation.

Another class of simple models, box ocean models, have been critical to understanding meridional ocean circulation, upwelling and mixing, among other processes (Stommel, 1961). In particular, they have suggested important climate questions to pursue by means of more sophisticated models, data, or both. Models and measurements established, however, the importance of the basic thermohaline circulation and the more complete meridional ocean circulation. With it, models for energy transport via diffusive processes were replaced by a more heterogeneous and dynamic mechanism. The Atlantic Meridional Overturning Circulation (AMOC), in particular, contributes a net energy transfer into the north Atlantic equivalent to several percent of the total incoming shortwave solar radiation incident to the region. Models of the meridional overturning circulation, from the simplest to the most detailed, agree that under present-day conditions the circulation is bistable (Rahmstorf, 2000; Rahmstorf et al., 2005). In addition to the thermally-dominated steady state that is currently ob-

served, a second, salinity-dominate steady state is also possible, with a much weaker circulation which flows in the direction opposite the present flow. It is clearly important to understand the interaction between this oceanic circulation and the distribution of sea ice.

Since the present-day AMOC transports heat into the north Atlantic, it tends to reduce the extent of sea ice. A strengthening of the circulation would then reduce ice cover, while a weakening would cause it to expand. The circulation itself is driven by wind stress in and near the Southern Ocean, as well as in part by mechanical mixing from tidal action Munk and Wunsch (1998), and it is sustained by variations in the density of circulating water as it exchanges ~~head~~ heat and fresh water with the atmosphere as it flows along the surface. As water flows northward along the surface through the tropics it is warmed, and its salinity increases as a result of excess evaporation. The increase in temperature decreases the water density, while the increase in salinity increases it. As the water passes to higher latitudes it cools, and freshens as precipitation exceeds evaporation. Again, the two effects tend to change the density in opposite directions. In the present configuration of the AMOC, the thermal effects dominate, so the water becomes denser as it moves through the subpolar latitudes, and ultimately sinks to return southward at depth.

The presence of sea ice affects the processes that change the density of circulating sea water at high latitudes. An ice cover isolates the water from the atmosphere and so cuts off the precipitation that otherwise would reduce the salinity of the water and lower the rate at which its density increases. It also insulates the water thermally from the atmosphere. This by itself would not have much effect on the water density, since the water temperature cannot fall below the freezing temperature anyways. However, it allows the atmosphere to become colder than it would be if it were in contact with the sea water. Heat transfer to the cold atmosphere through the ice layer results in freezing of sea water at the base of the ice. Brine rejection then increases the salinity and hence the density of the remaining water.

A simple model of ocean circulation with sea ice may be useful in studying the Snowball Earth episodes in the Neoproterozoic era. Since the discovery of geologic evidence suggesting that glaciation occurred in the tropics at least twice in the Neoproterozoic (Kirschvink, 1992; Hoffman and Schrag, 2002), some 710 and 635 million years ago (Ma), there has been substantial debate about whether the Earth was ever in a completely ice-covered Snowball Earth state (Lubick, 2002). These events are thought to have lasted several million years, raising such questions as how life could have survived a long period if the Earth were in a completely ice-covered state (McKay, 2000). Thus in trying to explain these signs of apparent tropical glaciation in the context of global climate dynamics, alternative hypotheses have been proposed that leave some portion of the ocean either free of ice, or covered only in thin ice (Hyde et al., 2000; Pollard and Kasting, 2005; Abbot and Pierrehumbert, 2010; Abbot et al., 2011).

Poulsen et al. (2001) counts among the first studies to suggest dynamic ocean heat transport is important to the Snowball Earth hypothesis. Using the fully coupled Fast Ocean-Atmosphere Model

(FOAM), initialized to Neoproterozoic parameter values to facilitate Snowball conditions, the authors found that a global ice cover was produced when using a mixed-layer ocean model that parameterized heat transport through diffusion. In fully coupled experiments with the ocean component, on the other hand, the ice margin would retreat to high latitudes. Other studies have considered the Snowball Earth problem in an EBM framework, with ocean heat transport typically parameterized by a diffusion process (Pollard and Kasting, 2005; Rose and Marshall, 2009). In particular, Pollard and Kasting (2005) examine the feasibility of a tropical thin-ice solution, incorporating detailed treatment of optical properties of ice and a non-linear internal ice temperature profile, as well as a separate snow layer and an evaporation minus precipitation term to facilitate surface melt/accumulation.

GCMs that have more detailed ocean physics have also been used to study the initiation of a Snowball Earth (Yang et al., 2012a, b). A recent study by Voigt et al. (2011) uses the state-of-the-art atmosphere-ocean model ECHAM5/MPI-OM to study the Snowball Earth scenario. They implement a Marinoan (635 Ma) land mask in their coupled GCM simulations, as well as the lower insolation of a younger, weaker sun. In addition to ocean dynamics, their study also included sea ice dynamics (albeit with thin ice) and interactive clouds. All three had previously been found to be essential for Snowball initiation (Poulsen et al., 2001; Poulsen and Jacob, 2004; Lewis et al., 2003, 2007). Voigt et al. (2011) were able to achieve Snowball initiation, and also to prevent Snowball initiation in the same setting by doubling carbon dioxide levels. Stability analysis of an EBM analog, based on the 0D model of global mean ocean temperature developed in Voigt and Marotzke (2010), indicates an insolation bifurcation point for Snowball Earth in the Marinoan setting of about 95-96% of pre-industrial levels, in agreement with their computational results. In their experiments that resulted in partial ice cover, the ice margin was around 30° to 40° latitude, with maximum stable sea ice extent of 55% of ocean cover observed in their experiments.

Sea ice in a global ice cover can be very thick, to the extent that flow by plastic deformation under its own weight should be considered. Thus its non-Newtonian fluid dynamics must be considered in addition to its thermodynamics. Goodman and Pierrehumbert (2003) (henceforth GP03) first considered these flow effects in the Snowball Earth scenario. (The same framework was used in Abbot and Pierrehumbert (2010) and Li and Pierrehumbert (2011) to transport dust to low latitudes in the Mudball scenario). Their model runs outside a global circulation model, using FOAM output for forcing data, and it has neither an active ocean component nor a parameterization for oceanic heat transport. They use the term 'sea glacier' to describe their modeled ice, to distinguish it from present-day sea ice, which only grows to thicknesses on the order of meters, and from land ice or ice shelves. The sea glacier is formed in the ocean, yet it achieves the thickness of a land ice sheet without the land-ice interface, and its non-Newtonian rheology is taken into account in the calculation of its flow. They are able to achieve both partial glaciation and a full Snowball state through changes in the atmospheric forcing (surface temperature and precipitation minus evaporation). They

find that the additional viscous flow term is highly effective at allowing the ice margin to penetrate low-latitude regions of melting, thus encouraging Snowball Earth initiation.

A recent study by Ashkenazy et al. (2013) found a dynamic ocean in a Snowball Earth scenario with strong circulation, in contrast to a stagnant ocean typically expected due to ice cover serving as an insulation layer to atmospheric forcing. Their model was forced with geothermal heat, which was spatially varying with a peak near the Equator, averaging to 0.1 W/m^2. In their 2D and 3D ocean simulations coupled with a 1D ice model extending upon that of GP03, they found that the ocean plays a larger role in determining ice thickness than the atmosphere, and that geothermal heat forcing plays a dominant role in ice-covered ocean dynamics. This was expanded upon in Ashkenazy et al. (2014), where a dynamic ocean with strong equatorial jets and a strong overturning circulation was found in simulations of a steady-state globally glaciated Earth.

Atmospheric dynamics and cloud cover undoubtedly play a large role in such climate systems, as demonstrated by Voigt et al. (2011). It is, however, difficult to isolate the role played by oceanic transport in these coupled simulations, due to the necessary inclusion of the complex dynamics of the atmosphere and cloud distribution as well as sea ice dynamics. In fact, in Voigt and Abbot (2012) it was found that ocean heat transport has no effect on the critical sea ice cover that leads to Snowball initiation. This motivated us to consider a simpler model that includes oceanic heat transport coupled to ice dynamics. We aim to extend the framework laid out in GP03 to include ocean heat transport effects, including under the ice layer. Realistic oceanic transport undoubtedly leads to highly non-uniform heat distributions, likely with local consequences on the global Snowball scenario. However, these local effects are beyond the scope of our study, and indeed beyond the scope of any low-dimensional model. By omitting atmospheric effects, we aim to get an assessment of the effects from oceanic heat transport alone.

The purpose of this paper is to investigate the interaction between sea ice and the meridional overturning circulation. By now there are several studies that have used complex circulation models to confirm that ocean transport is an important component of any explanation of how sea ice recedes and grows along with changes in forcing, albedo, biogeochemstry, etc. With a simple model, however, it is possible to efficiently test our understanding and propose questions critical to our being able to further understand the complexities of radiation, ice cover, and oceanic/atmospheric transport, such as the Snowball hypothesis.

To this end we have combined a one-dimensional energy balance model with a box model of the meridional overturning circulation and a dynamic ice component. Our model is described in detail in Section 2, a key element of which is the under ice heat exchange with the ocean. In Section 3 we present model results in different climate regimes. The sensitivity of the model to key parameterizations is studied in Section 4, and concluding remarks are in Section 5.

2 Model Description

Our model consists of a four-box ocean model with transport, similar to that first proposed by Stommel (1961), coupled to a one-dimensional EBM similar to that of Budyko (1969) and a dynamic model for sea ice coverage (GP03), and is depicted in Figure 1. The ocean component is a hemispheric model with thermohaline dynamics. While the ocean model uses a traditional transport equation for the salinity, it differs from traditional box models in the use of an energy conservation model to capture the temperature dynamics. This allows us to couple the ice and radiation components to the ocean dynamics. The ice layer is zonally averaged, so its thickness is taken to depend only on ~~colatitude~~ latitude θ and time t. The ice margin evolves dynamically, and we include non-Newtonian flow so that the model can accommodate an ice layer thick enough to be appropriate to Snowball conditions. The surface absorbs incoming solar radiation, with the an albedo which takes into account whether the surface is open ocean or ice, and emits long-wave radiation with a specified emissivity. Where ice overlies the ocean, heat conducts through the ice layer and is exchanged with the ocean at the ocean-ice interface, where melting and freezing can occur, while also supplying heat for redistribution through ocean circulation, a departure from typical EBMs. We also account for geothermal heat forcing, found to be the dominant forcing in a Snowball Earth ocean (Ashkenazy et al., 2013).

In addition to physical properties of ice and sea water, geometrical features of the ocean basin, and the distribution of insolation, there are three parameters which are important to our studies. In the energy balance model we model the greenhouse effective by including an effective emissivity, ε, in terms of modeling outgoing longwave radiation. The box model requires a hydraulic coefficient, k, which relates the strength of circulation to the densities of the water in the various boxes. The third parameter quantifies the thermal coupling between the sea ice layer and the water beneath; we express this as an effective thermal boundary layer thickness, D, with the rate of heat transfer from the water to the ice being proportional to the temperature difference between the box water and the base of the ice, divided by the thickness D. Among the issues we will investigate is the question of how, and indeed whether, the coupling relates the bistability of the energy balance model and the independent bistability of the box model.

2.1 Ocean and Energy Components

The ocean component of our model is similar to the one proposed by Griffies and Tziperman (1995) and Kurtze et al. (2010). Four boxes are used to represent the ocean in one hemisphere, from pole to Equator, with each box representing a zonal average across longitude. Referring to Figure 1, we define Box 1 as the tropical surface ocean box, Box 2 its polar counterpart, Box 3 below Box 2, and Box 4 below Box 1. The depth of the upper boxes is d_u and the depth of the lower boxes is d_l, with $d_u \ll d_l$. Boxes 2 and 3 extend from the pole at ~~colatitude $\theta = 0$~~ latitude $\theta = 90°$ to a fixed

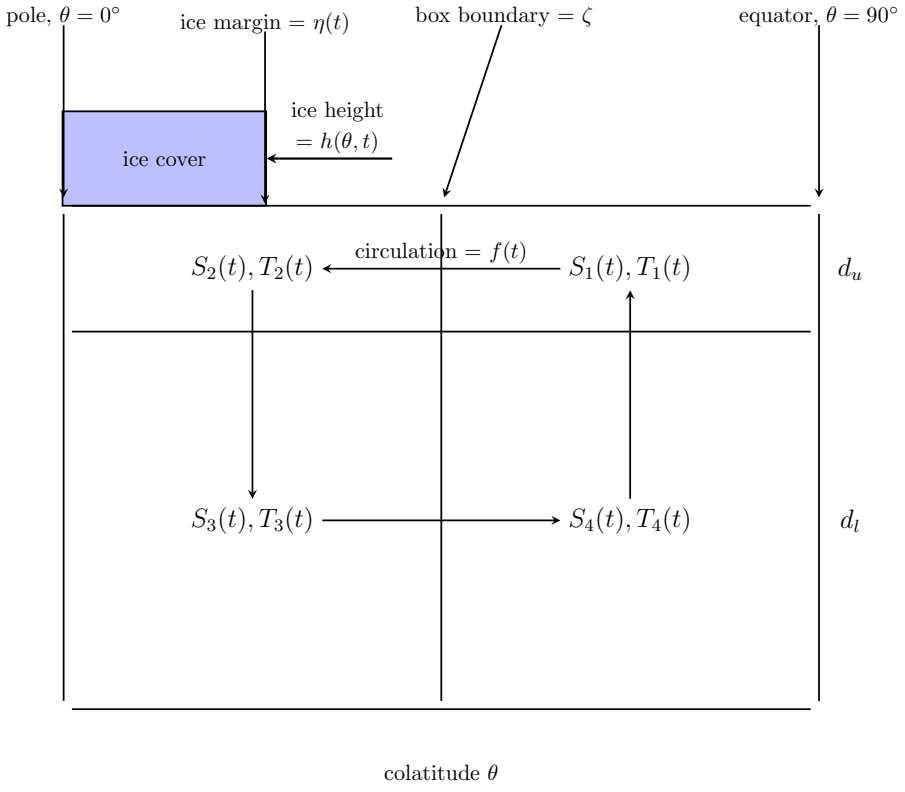

Figure 1. Hemispheric four-box arrangement. Boxes 1 and 2 are the surface ocean boxes of depth d_u, and Boxes 3 and 4 are the deep ocean boxes of depth d_l. The water in Box i has (well-mixed) salinity S_i and temperature T_i. The boundary between polar and equatorial boxes is at ~~colatitude~~ latitude ζ. Ice cover sits atop the surface boxes with height h and the ice margin at η. The arrows between the boxes represent density driven circulation f.

boundary at $\theta = \zeta$. Boxes 1 and 4 extend from $\theta = \zeta$ to the Equator at ~~$\theta = 90°$~~ $\theta = 0°$. We choose the ~~colatitude~~ latitude boundary ζ to be 45° simply because we are interested in investigating climate regimes ranging from global ice cover to zero ice cover, so there is no advantage in trying to confine the ice cover to a polar box only. We have found changing the location of this boundary within midlatitudes does not qualitatively affect our results. The dynamic ice margin is at $\eta(t)$, the ice cover thickness is given by $h(\theta, t)$, and its poleward meridional velocity is given by $v(\theta, t)$. Model parameter values, including geometric quantities pertaining to the box structure, are given in Table 2. For clarity, model variables will be subscripted with letters rather than numbers, using ut = upper tropic (Box 1), up = upper polar (Box 2), dp = deep polar (Box 3), and dt = deep tropic (Box 4).

Each box has a (well-mixed) temperature $T_j(t)$ and salinity $S_j(t)$, ~~$j = 1, ..., 4$~~ $j = st, sp, dp, dt$, which determine the density of each box by a linear equation of state

$$\rho_j(T_j, S_j) = \rho_0 \left[1 + \beta_S(S_j - S_0) - \beta_T(T_j - T_0)\right].$$

Here ρ_0 is a reference density corresponding to a reference temperature and salinity T_0, S_0. β_S and β_T are the expansion coefficients associated with salinity and temperature. The density-driven flow between the boxes is denoted by f, where we adopt the convention that $f < 0$ is surface poleward flow (from Box 1 to Box 2). As in Griffies and Tziperman (1995), the (buoyancy driven) transport rate is

$$f = k\left[\frac{d_u}{d_l}(\rho_{1ut} - \rho_{2sp}) + (\rho_{4dt} - \rho_{3dp})\right], \tag{1}$$

where $k = k_0 = 8 \cdot 10^4/\rho_0$ Sv is the hydraulic constant which governs the strength of the density driven flow. In Section 4.2 we explore the model's sensitivity to this parameter. The flux f is purely ~~thermohaline-driven~~thermohaline driven. We could modify this flux to include the effect of wind stresses in a crude manner by an additive correction to the flux, however, this has been omitted in this study.

The equations for each box's salinity and temperature will depend on the direction of the mean meridional flow. The salinity equations when $f < 0$, corresponding to poleward surface flow, are:

$$\begin{aligned}
V_1 \frac{dS_1}{dt}_{ut} \frac{dS_{ut}}{\delta t} &= |f|(S_{4dt} - S_{1ut}) + S_{1ut} 2\pi \int_{\zeta}^{\max\zeta,\eta\zeta} \int_{\max\zeta,\eta} \frac{\rho_w}{\rho_i} M(\theta) r_E^2 \sin\cos\theta d\theta, \\
V_2 \frac{dS_2}{dt}_{up} \frac{dS_{up}}{\delta t} &= |f|(S_{1ut} - S_{2up}) + S_{2up} 2\pi \int_{0}^{\min\zeta,\eta 90} \int_{\min\zeta,\eta} \frac{\rho_w}{\rho_i} M(\theta) r_E^2 \sin\cos\theta d\theta, \\
V_3 \frac{dS_3}{dt}_{dp} \frac{dS_{dp}}{\delta t} &= |f|(S_{2up} - S_{3dp}), \\
V_4 \frac{dS_4}{dt}_{dt} \frac{dS_{dt}}{\delta t} &= |f|(S_{3dp} - S_{4dt}).
\end{aligned} \tag{2}$$

Here V_j is the volume of the ~~j^{th}~~ j box, and $M(\theta, t)$ is the total production/melting rate of ice, with $M > 0$ corresponding to ice production and $M < 0$ corresponding to melting, described in Section 2.2. The terms involving the circulation rate f correspond to fluxes across the box boundaries. We assume that ice sits atop the surface ocean boxes, and that the mass of ice is much less than the total mass of ocean water. The surface ocean box volumes V_j are kept constant, and any changes to the deep ocean box volumes are negligible. An important assumption is that ice that is formed is fresh-water ice, and as such rejects brine into the ocean. The integral term represents the change in salinity due to net freshwater added/removed through ice melting/production. The bounds of integration represent the portion of each box covered in ice, and r_E is the Earth's radius. The ice component of the model serves as a saline forcing on the ocean box model component. There are similar equations for when ocean circulation is in the reverse direction.

In contrast to traditional Stommel box models, rather than using transport equations for the temperature we opt instead for thermal balance equations. The box temperatures change as heat transfers between boxes with the flow f, and as it transfers into the box via net radiation or conduction through

overlying ice. Thus for $f < 0$ the temperature equations are

$$c_w V_1 \frac{d(\rho_1 T_1)}{dt}_{ut} \frac{d(\rho_{ut} T_{ut})}{\delta t} = c_w |f| \left(\rho_{4dt} T_{4dt} - \rho_{1ut} T_{1ut} \right)$$
$$+ 2\pi \int_{\max\zeta,\eta}^{\pi/2} \left((1-\alpha_w) F_s(\theta) - \varepsilon\sigma {T_{1ut}}^4 \right) r_E^2 \sin\cos\theta d\theta$$
$$- \frac{\kappa_w}{D} (T_{1ut} - T_f) 2\pi \int_{\zeta}^{\max\zeta,\eta} r_E^2 \sin\cos\theta d\theta, \quad (3)$$

$$c_w V_2 \frac{d(\rho_2 T_2)}{dt}_{up} \frac{d(\rho_{up} T_{up})}{\delta t} = c_w |f| \left(\rho_{1ut} T_{1ut} - \rho_{2up} T_{2up} \right)$$
$$+ 2\pi \int_{\min\zeta,\eta}^{\zeta} \left((1-\alpha_w) F_s(\theta) - \varepsilon\sigma {T_{2up}}^4 \right) r_E^2 \sin\cos\theta d\theta$$
$$- \frac{\kappa_w}{D} (T_{2up} - T_f) 2\pi \int_{0}^{\min\zeta,\eta} r_E^2 \sin\cos\theta d\theta, \quad (4)$$

$$c_w V_3 \frac{d(\rho_3 T_3)}{dt}_{dp} \frac{d(\rho_{dp} T_{dp})}{\delta t} = c_w |f| (\rho_{2up} T_{2up} - \rho_{3dp} T_{3dp}) + F_g 2\pi \int_{0}^{\zeta} r_E^2 \sin\cos\theta d\theta d\theta, \quad (5)$$

$$c_w V_4 \frac{d(\rho_4 T_4)}{dt}_{dt} \frac{d(\rho_{dt} T_{dt})}{\delta t} = c_w |f| (\rho_{3dp} T_{3dp} - \rho_{4dt} T_{4dt}) + F_g 2\pi \int_{\zeta}^{\pi/2} r_E^2 \sin\cos\theta d\theta d\theta. \quad (6)$$

Here c_w is the ocean water heat capacity. The first term in each equation accounts for net energy accumulation due to fluxes across box boundaries. The second term in Equations (3) and (4) represents the radiative balance, in a similar form as appears in EBMs dating back to Budyko (1969). Here α_w is the ocean water albedo, and $F_s(\theta)$ is insolation, for which we use the parameterization of McGehee and Lehman (2012):

$$F_s(\theta) = \frac{342.95}{\sqrt{1-e^2}} \frac{2}{\pi^2} \int_0^{2\pi} \left[1 - (\cos\theta \sin\beta \cos\gamma - \sin\theta \cos\beta)^2 \right]^{1/2} d\gamma. \quad (7)$$

Here e is the eccentricity of the Earth's orbit (presently at 0.0167), β is the obliquity (presently at 23.5°), and γ is longitude. This parameterization is annually averaged (no seasonal cycle), but with time-dependent orbital parameters that allows for accounting for the Milankovitch cycles. However, in our results we found these were not strong enough to qualitatively affect the resulting model state, regarding the location of the ice margin, or Snowball Earth initiation or deglaciation, so only present day insolation values are used. The final terms in Equations (5) and (6) represent a uniform geothermal heating forcing~~of~~, with default $F_g = 0.05$ W/m^2, as in Ashkenazy et al. (2013).

In Equations (3) and (4), insolation is balanced by outgoing ~~long wave~~ longwave radiation, integrated over the exposed ocean portion of the box, where we assume blackbody radiation from the

surface using the full Stefan-Boltzmann law, with σ the Stefan-Boltzmann constant. As mentioned, ε is the effective emissivity, which is the ratio of outgoing longwave radiation emitted at the top-of-atmosphere to that emitted at the Earth's surface, and therefore represents the greenhouse effect. Thus atmospheric effects are distilled into this single parameter, which we will use as our control between climate states.

The last terms in (3) and (4) represent ice/ocean coupling by modeling heat transfer between the ocean box and its ice cover, a key component of our model. This includes the parameter D, having units of length, which parameterizes the under ice exchange of energy with the ocean and we refer to as the effective thermal boundary layer. We note that D is a key unconstrained parameter, which by default we set to $D = 0.05$m, and explore the model's sensitivity to this parameter in Section 4. Here κ_w is the sea water thermal conductivity, which we take to be constant, neglecting dependence on salinity and temperature.

The ocean heat transport in this model is then quantified as

$$H_{ocean} = f c_w \rho_w (T_{1ut} - T_{2up}).$$

As mentioned, the modeling approach taken herein does not include an active atmospheric component for the sake of keeping the model as simple as possible while focusing on the ice/ocean coupling in a reduced model sense. In this spirit, the parameter ε plays the role of the *net* forcing of the atmosphere on the ocean/ice system, including any heat / moisture transport within the atmosphere, which we consider to be out of our system.

2.2 Sea Ice Component

We largely follow the 'sea glacier' treatment of GP03 and later Li and Pierrehumbert (2011), with a few noted exceptions. The details of the rheology of sea glaciers are left to Appendix A. The equation for the ice thickness, by conservation of mass, is

$$\frac{\partial h(\theta,t)}{\partial t} + \nabla \cdot [v(\theta,t)h(\theta,t)] = M(\theta,t), \tag{8}$$

where $h(\theta,t)$ is ice thickness, $v(\theta,t)$ is meridional ice velocity, and $M(\theta,t)$ is the ice melting/production term. The equation for v is given by a Glen's flow law (GP03),

$$\nabla \cdot v(\theta,t) = \mu^n h(\theta,t)^n, \tag{9}$$

where μ is a temperature dependent ~~viscocity~~ viscosity parameter accounting for the non-Newtonian rheology of the ice, the details of which are left to Appendix A.

The ice melting/accumulation term $M(\theta,t)$ is a departure from the treatment of GP03. Ice melting or production can occur either from heat transferred through the ice from the surface, or from heat transferred through the ocean through the effective ice/ocean thermal boundary layer D, and is given by

$$LM(\theta,t) = \frac{\kappa_i}{\rho_i}\frac{T_f - T_s(\theta,t)}{h(\theta,t)} - \frac{\kappa_w}{\rho_w}\frac{T_{1,2}(\theta,t) - T_f}{D}, \tag{10}$$

where L is the latent heat of fusion of ice. When $M(\theta,t) > 0$, there is net accumulation of ice, and when $M(\theta,t) < 0$, there is net melting. The first term on the right side accounts for heat transfer through the ice, assuming a linear temperature profile in the ice from the surface $T_s(\theta)$ to the base at freezing T_f. The second term accounts for heat transfer with the ocean through the parameter D; an equivalent term appears in the energy budget for the ocean box temperatures in Equations (3) and (4). Since only average ocean box temperatures are computed by our model, to prevent an artificial and arbitrary jump in temperature across the box boundary from influencing the melting term, the step function surface temperature profile ~~$T_1(t), T_2(t)$~~ $T_{ut}(t), T_{up}(t)$ is regularized to a smooth $T_{1,2}(\theta,t)$ for use in Equation (10). Note that our model only accounts for melting and freezing at the base of the ice, and there are no terms that model melting at the upper surface or accumulation due to evaporation/precipitation forcing.

The ice surface temperature $T_s(\theta,t)$ is given by a primary radiative balance, as well as a term accounting for heat transfer through the ice. The (average annual) ice surface temperature $T_s(\theta)$ is given by

$$c_i \rho_i h(\theta) \frac{dT_s(\theta)}{dt} \frac{dT_s(\theta)}{\delta t} = F_s(\theta)(1-\alpha_i) - \varepsilon\sigma T_s(\theta)^4 + \kappa_i \frac{T_f - T_s(\theta)}{h(\theta)}, \tag{11}$$

where c_i is the specific heat, α_i the albedo, and κ_i the thermal conductivity of ice. The last term of Equation (11) accounts for heat transfer through the ice, as in Equation (10).

2.3 Model Setup

Settings for the parameters are listed in Table 2. The ocean component is run on a yearly time step, with the ice dynamics sub-cycled on a monthly time step. (This does not imply a seasonal cycle; rather we keep the insolation constant, as given in Equation (7)). For each ocean time step, we solve the set of differential equations for box temperatures and salinities (Equations (2) - (6)), and ice surface temperature (11) using a simple forward Euler method. At each ice time step, we solve (8) using a second-order upwind scheme after solving for the velocity in (9). We discretize our ~~longitudinal~~ latitudinal domain with 100 points, solving for ice thickness h and velocity v on staggered grids, and set $v = 0$ at the pole for the boundary condition in (9). We initialize the model in an ice free state, so any ice is formed through the model by equation (10). Following the setup of Griffies and Tziperman (1995), with initial box temperatures ~~$T_1 = 298°$ K, $T_2 = T_3 = T_4 = 273°$~~ $T_{ut} = 298°$ K, $T_{up} = T_{dp} = T_{dt} = 273°$ K and salinities ~~$S_1 = 36.5$ psu, $S_2 = 34.5$~~ $S_{ut} = 36.5$ psu, $S_{up} = 34.5$ psu, and ~~$S_3 = S_4 = 35$~~ $S_{dp} = S_{dt} = 35$ psu. Models that equilibrate to a climate state with no ice or a small ice cap typically reach an equilibrium climate steady state after 10,000 model years, ~~and the following results are at the end of 20,~~ however when the model reaches a state of global ice cover, a longer period of about 100,000 ~~model year runs~~years is needed before equilibrium is reached.

3 Results

As mentioned, we use the effective emissivity ε as a control between model climate states. We emphasize that, as we have no atmospheric heat transport or other atmospheric effects in our model other than this parameter to crudely account for greenhouse effects, we do not attribute physical meaning to this parameter value. With a choice of ~~$\varepsilon = 0.6$~~ $\varepsilon = 0.5$, which is estimated to be a reasonable value for current climate (Voigt et al., 2011), the model remains in an ice-free planet with a thermally driven poleward circulation of ~~≈ 29~~ ≈ 62.1770 Sv and associated heat transport ~~≈ 0.81~~ ≈ 3.7332 PW. We note the circulation strength is in line with results referenced in Griffies and Tziperman (1995) that give an approximate meridional circulation strength of 20 Sv from the coupled ocean-atmosphere model of NOAA's Geophysical Fluid Dynamics Laboratory (GFDL) model, and the ocean heat transport is in line with estimates for the North Atlantic ($\approx$ 1PW, Trenberth and Caron (2001)). The salinities of the boxes quickly mix and converge to roughly the same value of 35 psu. The equatorial surface box temperature settles to ~~$T_1 = 288.5°$~~ $T_{ut} = 304.0°$ K, whereas the other three boxes converge to a ~~common temperature of $T_2 = T_3 = T_4 = 281.7°$~~ closer temperature range with $T_{up} = 289.3, T_{dp} = 289.3$, and $T_{dt} = 289.4°$ K. Hence we have a strong, thermally dominated poleward circulation in this simulation. Depending on the choice of the ε parameter (which controls the radiative balance and parameterizes any atmospheric effects), the model can reproduce present day partial ice cover conditions, as well as Snowball Earth global ice cover conditions, as we will now describe.

3.1 Partial Glaciation

Raising the effective emissivity from ~~$\varepsilon = 0.6$~~ $\varepsilon = 0.5$ to $\varepsilon = 0.7$, we move to an equilibrium climate state with a small, stable ice cover. To determine the role of oceanic heat transport, we run the model with the circulation rate f set to zero for comparison against the full model run. Figure 2a,b shows the ice thickness and ice velocity profiles with and without ocean circulation, and we see the ocean circulation is effective at reducing ice thickness as well as pulling the ice margin north. Without the additional heat from the equatorial region moving poleward, the polar region remains cool, facilitating ice growth.

The ice cover is approximately ~~500m~~ 700m thick at the pole in the full model run, much thicker than current sea ice cover; however, this is consistent with partial glaciation results from GP03. It is because the ice is this thick that viscous flow effects need to be considered. There is a strong response in the ice velocity, largely due to the thicker ice cover when ocean circulation is not included, resulting in stronger viscous flow. The ice velocity reaches its maximum just before the ice margin (approximately ~~120 m~~2 km/yr in the full simulation). We also note the ice surface temperature seen in Figure 2c, calculated by Equation (11), is in line with the air surface temperature forcing used in

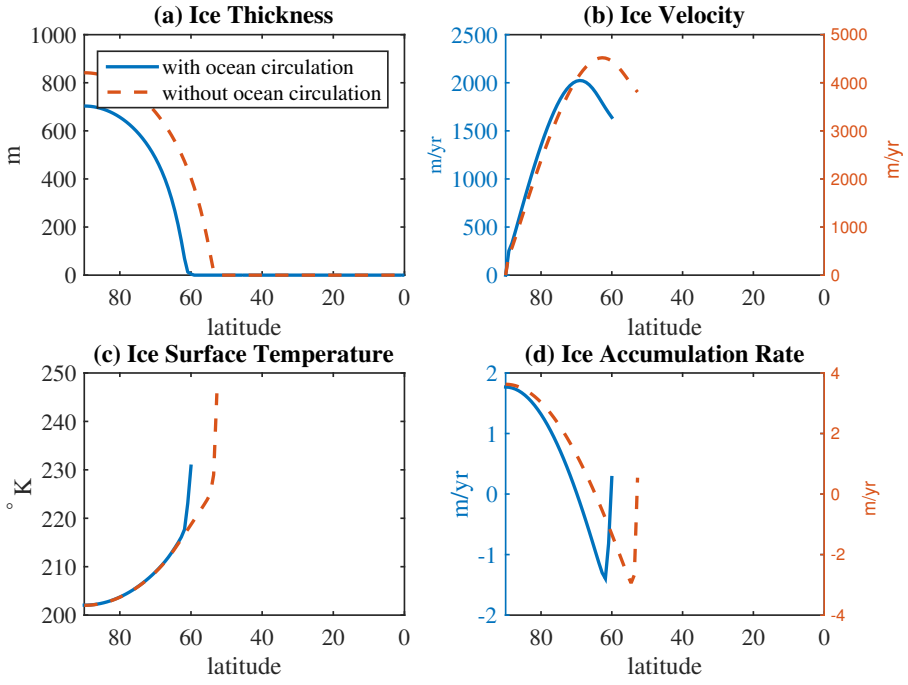

Figure 2. (a) Ice thickness h and (b) meridional velocity v profiles in partial ice cover scenario with effective emissivity $\varepsilon = 0.7$, with and without ocean circulation. Oceanic transport is seen to dramatically affect the ice predictions. (c) Ice surface temperature T_s and (d) ice basal accumulation rate in partial ice cover scenario with effective emissivity $\varepsilon = 0.7$, with and without ocean circulation. The accumulation term stabilizes the ice margin, and the model produces reasonable values of ice surface temperatures. M is positive over the region of ice cover indicating net accumulation of ice, and negative values of M beyond the ice margin indicate any ice present would be melted.

the experiments of GP03. In Figure 2d we see the accumulation term becoming negative near the ice margin, ~~indiciating~~ indicating a region of net melting that stabilizes the ice margin.

The steady state ocean circulation strength in this partial ice cover scenario is ~~≈ 26.3~~ ≈ 44.44 Sv, which is closer to the numerical results of the GFDL model referenced in Griffies and Tziperman (1995) than the ice-free run. As with the ice free runs, the box salinities quickly mix to the same value of approximately ~~35~~ 35.97 psu, while the surface equatorial box temperature settles to ~~$T_1 \approx 278.6°$~~ $T_{ut} \approx 281.6°$ K, and the other boxes mix to ~~$T_2 \approx T_3 \approx T_4 \approx 272.4°$~~ $T_{up} \approx 271.63, T_{dp} \approx 271.65, T_{dt} \approx 271.71°$ K. By increasing the effective emissivity ε, the model steady state ice profile moves smoothly ~~futher~~ further equatorward, until a large ice cap instability threshold is reached. When ice appears south of this instability threshold, the entire planet is covered in ice and a Snowball Earth state is reached.

3.2 Global Glaciation

To approximate the Neoproterozoic climate in our model, we lower insolation to 94% of its current value, accounting for a weaker, younger Sun (Voigt et al., 2011), and raise the geothermal heat flux from 0.05 to 0.08 W/m^2. Raising the effective emissivity from $\varepsilon = 0.7$ to ~~$\varepsilon = 0.85$~~$\varepsilon = 0.83$, we move from a climate state with a small, stable ice cover to global ice cover, a Snowball Earth, as shown in Figure 3. ~~With this global ice cover scenario, there is no region of net ice melting,as seen in Figure 3d, and without a manual change in forcing, such as an increase in the greenhouse effect until melting occurs,and ice will continue to accumulate without bound. However, the ice margin takes roughly 5,~~Global glaciation is reached within the first 10,000 model years, but then progresses slowly towards equilibrium between ice thickness and geothermal heat, so simulations in this regime are run for 500,000 years to reach steady state in the ice component. In the comparative run with no ocean circulation, the ~~Equator from initialization, and then produces a relatively neglible amount of ice . With continual positive net ice production, our assumption of ice being completely salt free produces ever increasing and unphysical salinity levels in the ocean boxes. However, since we have neglected salinity dependence of the freezing temperature, the model only depends on the salinity gradients between boxes, so unphysical salt content does not affect other aspects of the model.~~

~~(a) Ice thickness h and (b) velocity v profiles with 94% insolation and effective emissivity $\varepsilon = 0.85$, the Snowball Earth scenario. (c) Ice surface temperature T_s, which is seen to not be impacted by ocean circulation. (d) The ice accumulation term, while positive everywhere, has stabilized to small enough values that the profiles only change gradually after around 5,000 years~~

system will not reach steady state, as there is no geothermal heat flux reaching the ice layer, and as a result there is positive ice accumulation rate at all latitudes. In this scenario, the ocean circulation ~~reverses direction to a much weaker, saline-driven, equatorward circulation with a strength of approximately 4.9 Sv. Ocean circulation thus has a minor effect on the climate state, particularly on ice thickness and temperature profiles seen in Figure 3. The ocean box temperatures largely mix to a common value just above ocean freezing temperature, and the resulting flow is driven by salinity gradients. The ice thickness profile in Figure 3a shows a peak thickness at the pole of nearly 475m, reducing to about 175m near the Equator~~weakens to ≈ 16.5 Sv, with an associated heat transport of $\approx 6.27e-4$ PW. The resulting ice thickness is relatively uniform with a polar maximum of 2km, down to 1300m near the equator. The back-pressure term in the boundary condition for ice velocity in (A2) brings the ice velocity to zero at the Equator (Figure 3b), the effect of which is to move the maximum velocity ($\approx$ ~~55 m~~1 km/yr) to a location in the midlatitudes.

Examining the model results between these very different climate states of a small, stable ice cap at $\varepsilon = 0.7$ and Snowball Earth at ~~$\varepsilon = 0.85$~~$\varepsilon = 0.83$, we find a threshold where the model transitions. With an effective emissivity of ~~$\varepsilon = 0.84$~~$\varepsilon = 0.82$, the equilibrium climate state is near the large ice cap instability threshold, and we get a strong response from the ocean circulation. In Figure 4, we show the results of a simulation with and without ocean circulation dynamics. We observe in Figure

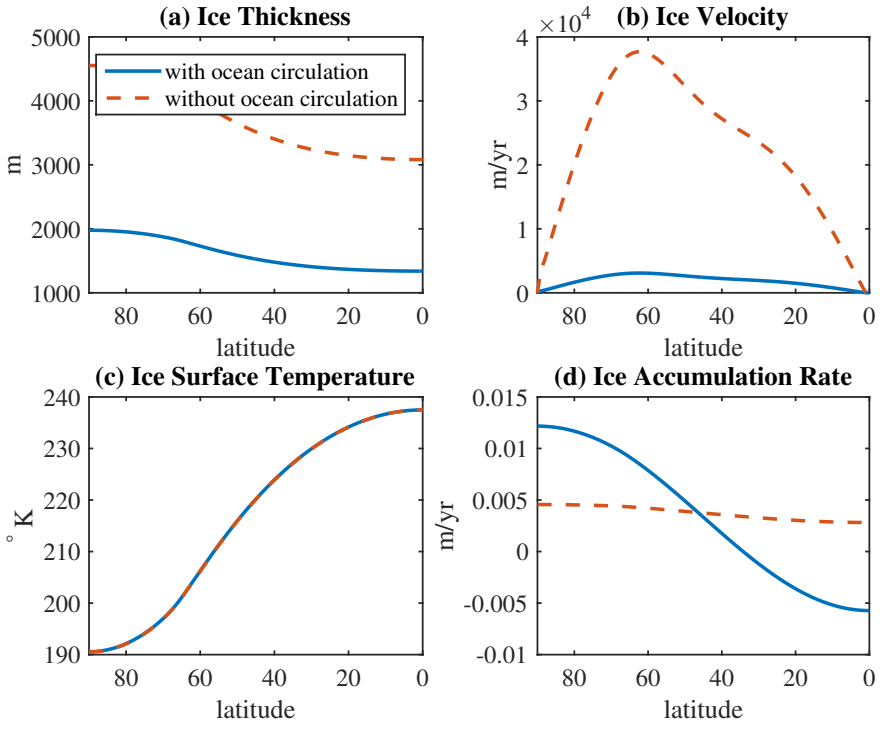

Figure 3. (a) Ice thickness h and (b) velocity v profiles with 94% insolation, $F_{geo} = 0.08$ W/m^2, and effective emissivity $\varepsilon = 0.83$, the Snowball Earth scenario. (c) Ice surface temperature T_s, which is seen to not be impacted by ocean circulation. In d), the simulation without ocean circulation cannot reach steady state due to geothermal heat not reaching the ice layer.

4a, that without oceanic heat transport, we get a Snowball Earth, but with oceanic heat transport, the ice line is held back from the Equator. As with the previous Snowball Earth state, the ocean circulation strength here, ~~2.7 Sv (equatorward) is considerably~~ 17.5 Sv (poleward) is weaker than in the small ice cap simulation. However even this weakened circulation, and thus weakened oceanic heat transport, is still enough to drive the climate into a Snowball state if turned off, demonstrating strong sensitivity in this regime.

4 Model sensitivity to ocean and atmosphere parameters

We have already seen the model sensitivity to the effective emissivity parameter ε, which we used to drive the model through vastly different climate states in Section 3. There are other key sensitivities the model exhibits, which we now discuss, namely in the ~~parameterizion~~ parameterization of energy transfer between the ocean and ice components, and the scaling strength of ocean circulation. By the nature of the large ice cap instability, the threshold effective emissivity of ~~$\varepsilon = 0.84$~~ $\varepsilon = 0.82$ seen in

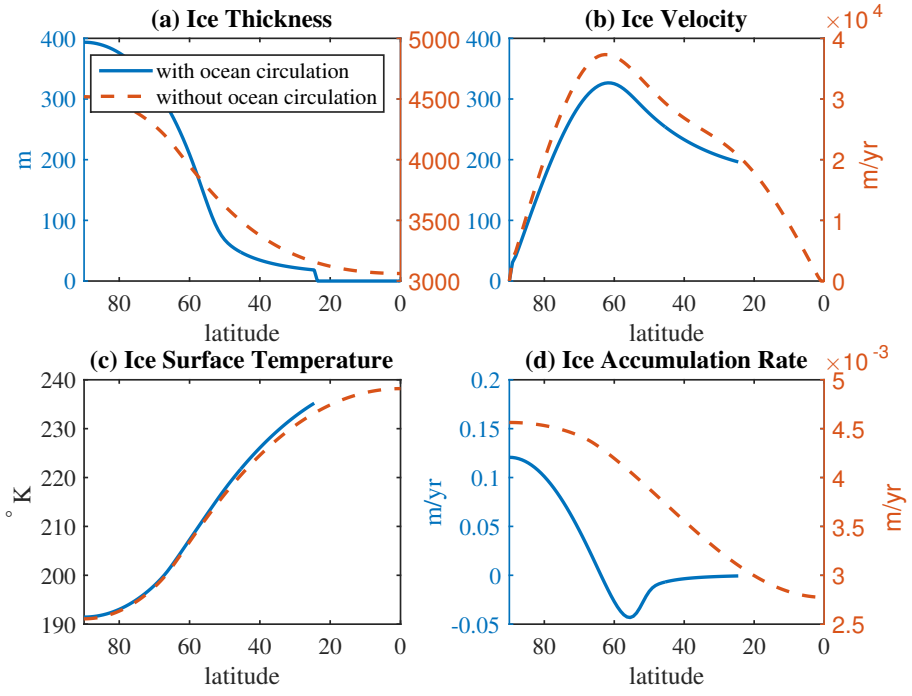

Figure 4. (a) Ice thickness h and (b) velocity v profiles with 94% insolation and ~~$\epsilon = 0.84$~~$\epsilon = 0.82$, with and without ocean circulation. We note neglecting oceanic heat transport leads to drastically different global climate states. (c) Ice surface temperature T_s and (d) ice basal accumulation M, which without oceanic heat transport is positive everywhere.

Section 3.2 is sensitive to the parameter choices representing these key processes. We also explore the model's bistability in the small ice cap and large ice cap instabilities.

4.1 Ocean / ice energy transfer parameterization

The parameter D is responsible for parameterizing the transfer of energy between the ocean and ice systems, a so called effective thermal boundary layer, and is the least constrained parameter in our model. It appears in equations for the surface ocean box temperatures (3), (4) as well as in ice melting/production (10). The role of D has competing effects in these two equations. For the ocean box temperatures, D appears in the term corresponding to energy loss due to the presence of the ice cover, and thus increasing D cools the ocean. However this energy loss is balanced in the system by the ice melting/production term, where increasing D encourages melting. In the limiting case of $D = 0$, the ocean and basal ice would be forced to the same temperature, and increasing D further insulates the ocean from the ice, by slowing the heat transfer between the two component. There are also other feedbacks in the system, notably the indirect effect of D on the strength of the ocean circulation, and thereby oceanic heat transport, which we have already seen can strongly affect ice cover.

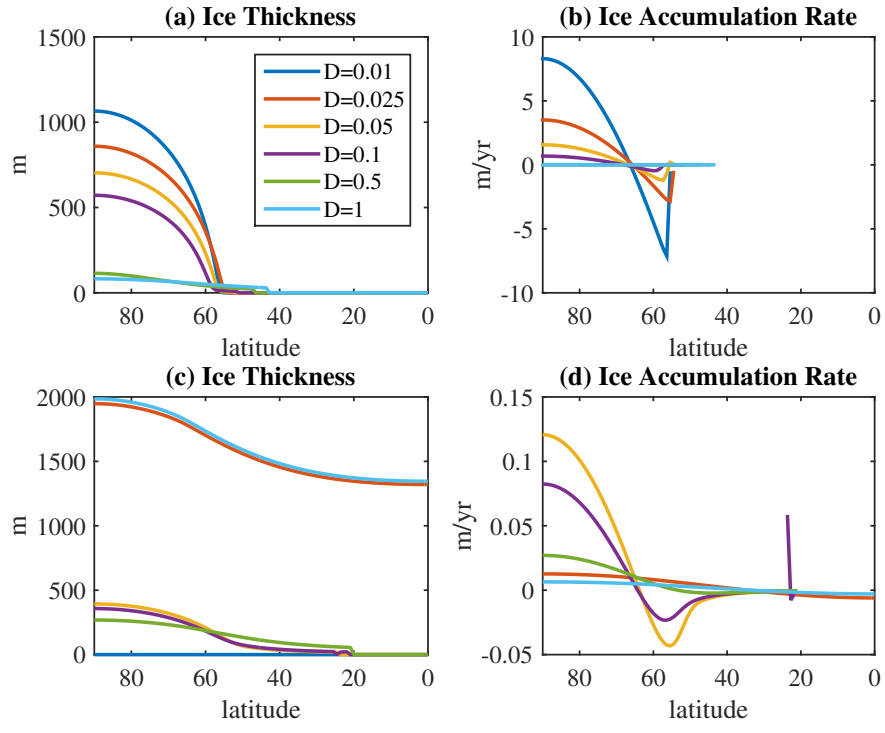

(a)

Figure 5. Effect of D parameter on equilibrium climate state, small ice cap regime ($\varepsilon = 0.75$, top), and large ice cap regime (~~$\varepsilon = 0.84$ and~~ $\varepsilon = 0.82$, 94% insolation, $F_{geo} = 0.08 W/m^2$ bottom). There is particularly strong response in the resulting melting / accumulation term which was used to constrain the value of D. Furthermore, the instability near the large ice cap threshold is reflected in nearby values of D to the default $D = 0.05$ resulting in global ice cover for ~~$\varepsilon = 0.84$~~$\varepsilon = 0.82$.

We explore the model's sensitivity to values of this parameter over two orders of magnitude in Figure 5 in both the small ice cap regime ($\varepsilon = 0.75$), and near the large ice cap instability (~~$\varepsilon = 0.84$~~$\varepsilon = 0.82$, insolation at 94% current values, $F_{geo} = 0.08 W/m^2$), showing ice thickness profiles and ice melting / ~~accummulation~~ accumulation rate at the end of a ~~20~~50,000 year run to equilibrium. In the small ice cap regime, increasing D steadily reduces ice thickness, though the ice margin remains in a small high latitude range across changes in D, apart from the large end of the range, where the margin pushes further equatorward. The ocean circulation (poleward) also steadily reduces with increased D, from ~~20~~ 32.9 Sv circulation with $D = 0.01$ down to ~~10~~ 20.5 Sv circulation for $D = 1$. There is, however, a strong response in the ice melting / accumulation term, where large values of D yield small magnitude melting terms. This proved to be critical in melting excess ice, which we saw in our experiments with changing solar forcing discussed below in Section 4.3.

~~The large ice cap threshold emissivity for D = 0.05 is $\varepsilon = 0.84$, and we see the instability reflected in that the other values of D result in a global ice cover. There is an interesting divide in ocean circulation in the large ice cap regime, where the large tested values of $D = 0.5, 1$ result in ≈ 7.5~~

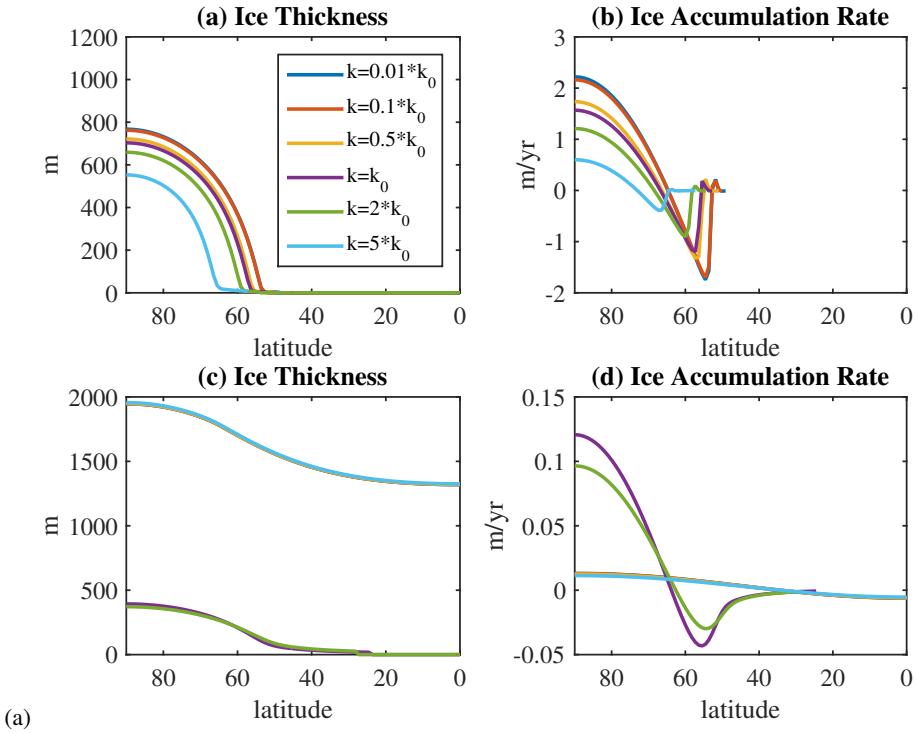

(a)

Figure 6. Effect of k_0 parameter on small ice cap regime (top) and large ice cap regime (bottom). Smaller circulation constants reduce heat transport from the tropics to the poles, thereby facilitating ice growth. The large ice ~~capt~~ cap instability is again reflected in the sensitivity to changes to the ~~circulation~~ hydraulic constant, with the shown deviations resulting in Snowball Earth.

~~Sv poleward circulation, whereas the other D values result in ≈ 3 - 5 Sv equatorward circulation. Note that in Figure 5c, we see different behavior in the ice accumulation, and thus freshwater forcing, term associated with these different directions of circulation. The more spatially uniform accumulation terms, $D = 0.5, 1$ are associated with poleward circulation, and the other global ice accumulation terms share a similar shape increasing with colatitude. Thus we see both directions of ocean circulation are consistent with the Snowball Earth scenario (albiet only demonstrated with different parameters so far). The sensitivity of the model results to this simple parameterization of heat flux between the ocean and ice cover demonstrates the importance of this exchange in the heat budget.~~

4.2 ~~Circulation~~ Hydraulic constant

The default value of the ~~circulation~~ hydraulic constant $k = k_0$ in (1) from Griffies and Tziperman (1995) results in a circulation strength of $\approx$ ~~20~~ 32.7 Sv, in line with estimates of present-day mean meridional ocean circulation. This may not be appropriate for the Neoproterozoic, warranting an examination of the sensitivity of the model to changes to this parameter, explored in Figure 6. We

again show results for the same experimental setups as in Section 4.1. Here we see a stronger effect on the ice margin in the small ice cap regime, where smaller ~~circulation~~ hydraulic constants reduce heat transport from the tropics to the poles, thereby facilitating ice growth (note circulation always remains poleward in this regime). In the large ice cap regime, we again see the sensitivity of the large ice cap instability, as deviating from the default circulation strength constant, in either direction moves the threshold emissivity away from ~~$\varepsilon = 0.84$~~$\varepsilon = 0.82$, and the resulting climate state is a Snowball Earth. ~~For the Snowball Earth states, there is also an interesting divide in direction of circulation, in that all circulations are actually poleward, ranging from 16 Sv to 1 Sv, except for the $k = 2 * k_0$ case, where the Snowball Earth resulting circulation is equatorward at 7 Sv. In Figure 6 we see the same association of accumulation rate profiles with circulation direction, where elongated S shape for $k = 2 * k_0$ corresponds to equatorward circulation, and the other more spatially uniform profiles correspond to poleward circulation.~~

4.3 Model Bistability

As discussed, a well-known feature of EBMs are hysteresis with respect to radiative forcing. To study this in our model, we setup experiments to investigate the hysteresis loop in the small ice cap instability and the large ice cap instability. In the small ice cap case, we began with conditions that resulted in a small ice cap, gradually increased radiative forcing by decreasing the emissivity ε until the ice cap melted away, and then increased ε to its starting value. With each incremental change in ε, the model is run for ~~10~~50,000 years to ensure that the model is in equilibrium. A similar experiment was run for the large ice cap case, except with the forcing changes in cooling first, until Snowball Earth is reached, and then subsequent warming. The results of these experiments are shown in Figure 7.

The expected hysteresis loops in each scenario manifest themselves in the left column of Figure 7. In the small ice cap case, The ice margin begins with $\varepsilon = 0.7$ near ~~17~~ 60 ° ~~colatitude~~latitude, and following the red path through decreasing ε, we see the ice cap abruptly change from a margin at ~~10° colatitude~~80° latitude, to completely disappear at ~~$\varepsilon = 0.6$~~$\varepsilon = 0.55$. As the forcing is then cooled through the blue path, the model remains ice free until the appearance of a small ice cap near ~~$\varepsilon = 0.68$~~$\varepsilon = .62$, returning to its starting location at $\varepsilon = 0.7$. Looking at the response of the ocean circulation through the experiment, there is a small response in the strength of circulation in the hysteresis loop. As alluded to in Section 4.1, this behavior was actually used to constrain the value of $D = 0.05$, as larger values of D did not yield adequate melting rates to melt ice once it appeared, resulting in very large hysteresis loops. It is worth noting that the hysteresis loop in this model is present with only ocean heat transport, in the absence of an explicit atmospheric heat transport parameterization, which has previously been found to be necessary for such bistability Held and Suarez (1974)

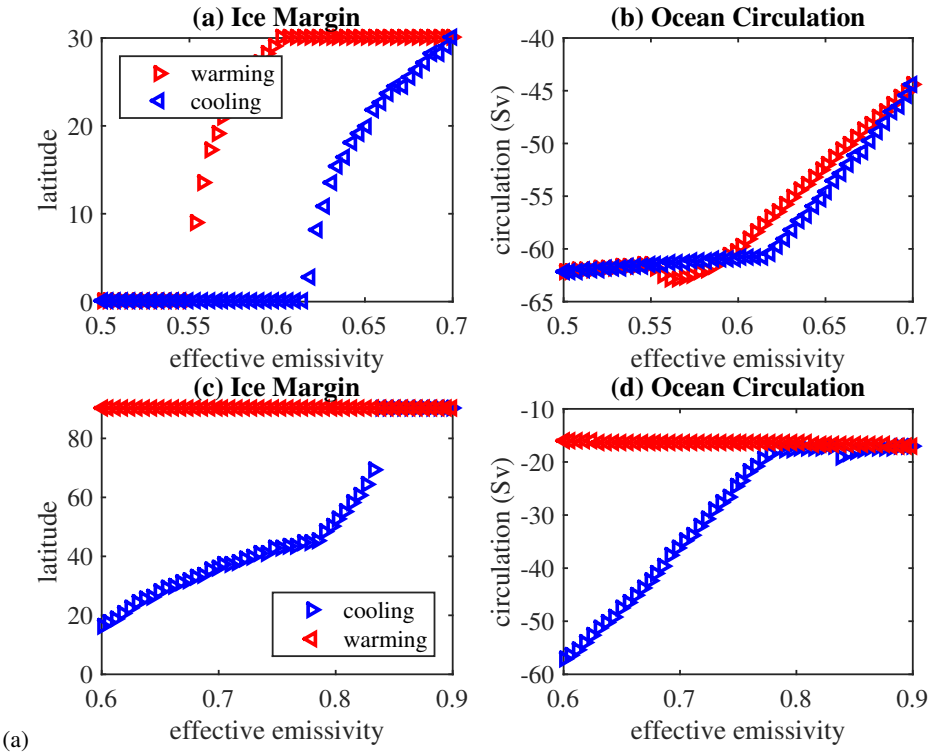

(a)

Figure 7. Hysteresis experiments, radiative forcing. Top, small ice cap regime: forcing changes in ε, warming first ($\varepsilon = 0.7 \mapsto 0.5$), then cooling ($\varepsilon = 0.5 \mapsto 0.7$). Resulting ice margin (left) and circulation (right) are shown, demonstrating a hysteresis loop in the ice margin. Bottom, large ice cap regime: with insolation set to 94% present values, forcing changes in ε, cooling first to achieve Snowball Earth ($\varepsilon = 0.6 \mapsto 0.9$), then subsequent warming ($\varepsilon = 0.9 \mapsto 0.6$). Strong hysteresis loop is seen in the ice margin, as the model is unable to escape Snowball Earth even as radiative forcing is raised to levels associated to ice free states, although strong enough increases in radiative forcing will eventually melt ice away from global ice cover. Circulation remains poleward, ever increasing through the Snowball Earth state manual radiative forcing increase.

In Figure 7c, we see the familiar large ice cap instability hysteresis loop, where as the climate is cooled through increasing ε, the ice margin gradually increases until the large ice cap instability is reached near ~~70° colatitude~~20° latitude, and beyond which Snowball Earth is reached. ~~Notable is that in this gradual cooling, the ocean circulation remains poleward through the large ice cap instability to Snowball Earth, the opposite direction that was seen for the same parameters and forcing in Section 3.2 when the model was initialized and run in the regime to produce large ice cap or Snowball conditions. Thus here we have true bistability of the direction of ocean circulation in the large ice cap and Snowball Earth regime.~~ As the climate is subsequently warmed, Snowball Earth is maintained, but notably the ocean circulation remains poleward, ~~continuining~~ continuing to transport heat to the poles, and in fact with a strong increase in warming (up to $\varepsilon = 0.4$), Snowball Earth is escaped in the model.

(a)Hysteresis experiments, circulation strength constant. Top, small ice cap regime: forcing changes in k, weakening first ($k = k_0 \mapsto 0$), then strengthening ($k = 0 \mapsto k_0$). Bottom, large ice cap regime: forcing changes in k, weakening first ($k = k_0 \mapsto 0$), then strengthening back to the default circulation constant ($k = 0 \mapsto k_0$). In the small ice cap experiment, while the ice margin does not melt back from its furthest extent, the resulting ocean circulation actually remains in line as the strength constant is dialed down to 0 and back up again. In the large ice regime, weakening the circulation causes a collapse to Snowball Earth, which is then inescapable as manually increasing the circulation constant only furthers the equatorward circulation.

As there is also present concern of a collapse of the AMOC, we also wanted to see the effect of changing the ocean circulation forcing to weaken to zero, then increase again. For this we manually changed the circulation constant k in Equation 1, weakening k from k_0 to 0, and then back to k_0. In Figure **??**, we see that while the resulting circulation follows a very close path through weakening and strengthening again, despite the ice margin not retreating during the strengthening phase. The more interesting case however is the large ice cap scenario, where weakening the circulation constant sends the model into a Snowball Earth, which is then inescapable as manually increasing the circulation constant only furthers the equatorward circulation.

5 Conclusions

We have presented a low dimensional conceptual climate model consistent with elements of classical low dimensional models that is able to reproduce both present day, partial ice cover climate, as well as a Snowball Earth global ice cover climate. The radiative balance terms similar to those in EBMs produce states of ice cover consistent with classical EBM results of two stable solutions, a small ice cover and a global ice cover, as well as an unstable solution, a large but finite ice extent. The ocean box model produces ocean states in two circulation regimes: a strong, poleward, thermally driven circulation, as well as a weaker, equatorward, saline driven circulation. A summary of these results is given in Table 1.

Our primary interest is investigating the role of dynamic ocean circulation in the initiation of Snowball Earth, particularly in the large ice cap instability. We find in parameter regimes where there is no ice or a small ice cap, the ocean circulation is expectedly thermally dominated and poleward. Moving through parameter space to larger ice margins, the ocean circulation weakens, until ultimately reversing direction near the large ice cap instability, resulting in a Snowball Earth scenario and a weak, equatorward circulation. Discounting ocean circulation altogether allows for easier transition into global ice cover. We find, together with the effective emissivity which parameterizes the atmospheric component, that the energy transfer between the ice and ocean components plays a crucial role in determining the model's resulting climate state.

The results from our ice component are largely in line with those of GP03, in both ice thickness and position of the ice margin, despite some key differences in modeling approach. There is a notable difference in the ice velocity, however, in that our computed ice velocities are an order of magnitude less those reported in GP03. One possible reason for this is that the viscosity parameter μ, which GP03 are only required to calculate once due to a static surface temperature forcing, is recalculated in our model in response to the dynamic surface temperature in (11). Our steady state surface temperature (shown in Figure 4) is cooler than the forcing used in GP03 partial glaciation case, and thus our cooler surface temperature creates more viscous ice, slowing down ice flow. The ice thickness profiles in our Snowball experiments vary smoothly by a couple hundred meters from pole to Equator, in contrast to sea glacier models that obtain a more uniform thickness in Snowball state, as in Li and Pierrehumbert (2011). Our results also qualitatively agree with that of Pollard and Kasting (2005) (e.g. ice thickness, velocity, ice accumulation rates, surface temperature) in the steady state Snowball Earth scenario, with the notable exception of a sharper decline in tropical ice thickness, and while we are confident that adopting their more developed ice model would not significantly change the results of our model presented here in the Snowball Earth scenario (apart from a thinner tropical ice), it would certainly be of interest to study transient behavior and parameter ranges that lead to climate regimes other than Snowball Earth.

The ocean in our Snowball scenario has a considerably weaker circulation strength of ~~4.9~~ 16 Sv than present-day estimates, and while this is not indicative of a stagnant ocean, it is not as strong as the circulation strengths of approximately 35 Sv that were achieved in the study of Ashkenazy et al. (2013). Their 2D simulations allowed for resolution of both vertical mixing and horizontal eddies, and while they also did not have land in their simulations, they did have an underwater ocean ridge that had a highly localized and higher strength geothermal heat forcing corresponding to a spreading center, which, together with strong vertical salinity profiles, drove the strong circulation.

The main conclusion we reach from this study is that ocean circulation and its associated heat transport play a vital role in determining the global climate state and ice cover. We have seen in the partial glaciation case that the ocean circulation severely inhibits ice growth, and we have seen in the near global glaciation case that even in that state's severely weakened ocean circulation, lack of oceanic transport leads to a drastically different Snowball Earth state. In particular, our study found that both heat flux between the ice and ocean, and the value of the circulation constant that controls circulation strength (tuned to present day conditions) played a crucial role in determining the global climate state. Not only do we find bistability in the small and large ice cap instability regimes with regards to radiative forcing, ~~we also find that both thermally driven poleward, and saline driven equatorward circulations are consistent with a Snowball Earth scenario, a bistability arising from indirect freshwater forcing through the model's ice melting / accumulation term.~~

Our inclusion of a simple parameterization of under-ice ocean heat transport, mediating dynamic oceanic heat transfer not present in traditional EBM diffusive heat transport models is here found

to be crucial in determining the steady state climate regime. This warrants further investigation in a GCM setting, to examine the role played by thermal processes in the ice and ocean that account for heat transport in the sub-ice cover layer. To be more direct, we find that oceanic heat transport is crucial to understanding Snowball initiation; that the ice cover affects it significantly; that the results are sensitive to the water-ice thermal coupling and the factors driving the circulation; and that it is therefore worthwhile to use GCMs to investigate these factors in detail.

While atmospheric effects were largely neglected for simplicity and because our focus was on the role of oceanic heat transport in the Snowball Earth setting, including an atmospheric component would be the natural progression of this work, particularly an precipitation - evaporation component that would facilitate ice surface melting/accumulation, though it is worth noting that we were able to reproduce both present day and Snowball Earth conditions without a precipitation - evaporation forcing.

Appendix A: Sea glacier rheology

Ice is a non-Newtonian fluid, which deforms under its own weight by compressing vertically and stretching laterally, causing lateral ice flow. The flow rate, first suggested by Glen (1955), has been empirically found to be a power law relating strain rate $\dot{\epsilon}$ and stress $\tilde{\sigma}$,

$$\dot{\epsilon} = A\tilde{\sigma}^n,$$

where A, n are rheological parameters. This was extended to a floating ice-shelf model byWeertman (1957), and later by Macayeal and Barcilon (1988). From this work, GP03 use a Glen's flow law to describe ice velocity $v(\theta,t)$ in terms of rheological parameters:

$$\nabla \cdot v(\theta,t) = \mu^n h(\theta,t)^n, \tag{A1}$$

with $n = 3$, where μ is a viscosity parameter, given by Weertman (1957):

$$\mu = \frac{1}{4}\rho_i g \left(1 - \frac{\rho_i}{\rho_w}\right) \overline{A^{1/n}}.$$

Here ρ_i, ρ_w are the densities of ice and water, g is the acceleration due to gravity, and $\overline{A}$ is the depth-averaged Glen's flow law parameter (Sanderson, 1979; Goodman and Pierrehumbert, 2003; Li and Pierrehumbert, 2011), given by (suppressing dependence on ~~colatitude~~ latitude θ)

$$\overline{A} = \frac{1}{h}\int_{-h}^{0} A_0 \exp\left(\frac{-Q}{RT(z)}\right) dz.$$

R is the gas constant, A_0 and Q are parameters split by a temperature boundary (as in Barnes et al. (1971), Goodman and Pierrehumbert (2003), Li and Pierrehumbert (2011)) given in Table 2, and $T(z)$ is the vertical temperature profile through the ice.

In the event that ice reaches the Equator, we follow the treatment of GP03 to bring the velocity at the Equator to zero through a balance of a back-pressure term from the force of ice colliding with ice from the other hemisphere (assuming symmetry of Northern and Southern hemispheres). They found the appropriate version of (A1) in this case is

$$\frac{\partial v(\theta,t)}{\partial \theta} + v(\theta,t)\cot\theta = r_E \mu^n \left(h(\theta,t) - \frac{b}{h(\theta,t)} \right)^n ,$$

where the back-pressure constant b satisfies

$$\begin{aligned} 0 &= v(\theta = 90^\circ) \\ &= r_E \int_0^{2\pi} \mu^n \left(h(\theta,t) - \frac{b}{h(\theta,t)} \right)^n \sin\theta d\theta, \end{aligned} \tag{A2}$$

which we solve by Newton's method.

Acknowledgements. Funding for this work was received from GoMRI/BP and from NSF DMS grant 0304890. JMR also wishes to thank the American Institute of Mathematics, an NSF-funded institute where some of this research was done. The authors also wish to thank Raymond Pierrehumbert and Dorian Abbot for stimulating conversations.

References

Abbot, D. S. and Pierrehumbert, R. T.: Mudball: Surface dust and Snowball Earth deglaciation, Journal of Geophysical Research: Atmospheres (1984–2012), 115, 2010.

Abbot, D. S., Voigt, A., and Koll, D.: The Jormungand global climate state and implications for Neoproterozoic glaciations, Journal of Geophysical Research: Atmospheres (1984–2012), 116, 2011.

Armour, K., Eisenman, I., Blanchard-Wrigglesworth, E., McCusker, K., and Bitz, C.: The reversibility of sea ice loss in a state-of-the-art climate model, Geophysical Research Letters, 38, 2011.

Ashkenazy, Y., Gildor, H., Losch, M., Macdonald, F. A., Schrag, D. P., and Tziperman, E.: Dynamics of a Snowball Earth ocean, Nature, 495, 90–93, 2013.

Ashkenazy, Y., Gildor, H., Losch, M., and Tziperman, E.: Ocean Circulation under Globally Glaciated Snowball Earth Conditions: Steady-State Solutions, Journal of Physical Oceanography, 44, 24–43, 2014.

Barnes, P., Tabor, D., and Walker, J.: The friction and creep of polycrystalline ice, Proceedings of the Royal Society of London. A. Mathematical and Physical Sciences, 324, 127–155, 1971.

Budyko, M. I.: The effect of solar radiation variations on the climate of the Earth, Tellus, 21, 611–619, 1969.

Glen, J.: The creep of polycrystalline ice, Proceedings of the Royal Society of London. Series A, Mathematical and Physical Sciences, pp. 519–538, 1955.

Goodman, J. and Pierrehumbert, R.: Glacial flow of floating marine ice in Snowball Earth, Journal of Geophysical Research, 108, doi:doi:10.1029/2002JC001471, 2003.

Griffies, S. and Tziperman, E.: A Linear Thermohaline Oscillator Driven by Stochastic Atmospheric Forcing, Journal of Climate, 8, 2440–2453, 1995.

Held, I. M. and Suarez, M. J.: Simple albedo feedback models of the icecaps, Tellus, 26, 613–629, 1974.

Hoffman, P. F. and Schrag, D. P.: The Snowball Earth hypothesis: testing the limits of global change, Terra Nova, 14, 129–155, 2002.

Hyde, W. T., Crowley, T. J., Baum, S. K., and Peltier, W. R.: Neoproterozoic Snowball Earth simulations with a coupled climate/ice-sheet model, Nature, 405, 425–429, 2000.

Kirschvink, J. L.: Late Proterozoic low-latitude global glaciation: the Snowball Earth, 1992.

Kurtze, D. A., Restrepo, J. M., and Dittmann, J.: Convective adjustment in box models, Ocean Modelling, 34, 92–110, 2010.

Lewis, J., Weaver, A., and Eby, M.: Snowball versus slushball Earth: Dynamic versus nondynamic sea ice?, Journal of Geophysical Research, 112, C11 014, 2007.

Lewis, J. P., Weaver, A. J., Johnston, S. T., and Eby, M.: Neoproterozoic snowball Earth: Dynamic sea ice over a quiescent ocean, Paleoceanography, 18, 2003.

Li, D. and Pierrehumbert, R.: Sea Glacier flow and dust transport on Snowball Earth, Geophysical Research Letters, doi:doi:10.1029/2011GL048991, 2011.

Lubick, N.: Paleoclimatology: Snowball Fights, Nature, 417, 12–13, 2002.

Macayeal, D. and Barcilon, V.: Ice-shelf response to ice-stream discharge fluctuations: I. Unconfined ice tongues, Journal of Glaciology, 34, 1988.

McGehee, R. and Lehman, C.: A Paleoclimate Model of Ice-Albedo Feedback Forced by Variations in Earth's Orbit, SIAM Journal on Applied Dynamical Systems, 11, 684–707, 2012.

McKay, C.: Thickness of tropical ice and photosynthesis on a Snowball Earth, Geophysical research letters, 27, 2153–2156, 2000.

Munk, W. and Wunsch, C.: Abyssal recipes II: energetics of tidal and wind mixing, Deep Sea Research Part I: Oceanographic Research Papers, 45, 1977–2010, 1998.

Pollard, D. and Kasting, J. F.: Snowball Earth: A thin-ice solution with flowing sea glaciers, Journal of Geophysical Research: Oceans (1978–2012), 110, 2005.

Poulsen, C. J. and Jacob, R. L.: Factors that inhibit snowball Earth simulation, Paleocenography, 19, doi:10.1029/2004PA001056, 2004.

Poulsen, C. J., Pierrehumbert, R. T., and Jacob, R. L.: Impact of ocean dynamics on the simulation of the Neoproterozoic Snowball Earth, Geophysical research letters, 28, 1575–1578, 2001.

Rahmstorf, S.: The thermohaline ocean circulation: A system with dangerous thresholds?, Climatic Change, 46, 247–256, 2000.

Rahmstorf, S., Crucifix, M., Ganopolski, A., Goosse, H., Kamenkovich, I., Knutti, R., Lohmann, G., Marsh, R., Mysak, L. A., Wang, Z., et al.: Thermohaline circulation hysteresis: A model intercomparison, Geophysical Research Letters, 32, 2005.

Rose, B. E. and Marshall, J.: Ocean heat transport, sea ice, and multiple climate states: Insights from energy balance models, Journal of the Atmospheric Sciences, 66, 2828–2843, 2009.

Sanderson, T.: Equilibrium profile of ice shelves, Journal of Glaciology, 22, 1979.

Sellers, W. D.: A global climate model based on the energy balance of the earth-atmosphere system, Journal of Applied Meteorology, 8, 392–400, 1969.

Stommel, H.: Thermohaline convection with two stable regimes of flow, Tellus, 13, 224–230, 1961.

Trenberth, K. E. and Caron, J. M.: Estimates of meridional atmosphere and ocean heat transports, Journal of Climate, 14, 3433–3443, 2001.

Voigt, A. and Abbot, D.: Sea-ice dynamics strongly promote Snowball Earth initiation and destabilize tropical sea-ice margins., Climate of the Past, 8, 2012.

Voigt, A. and Marotzke, J.: The transition from the present-day climate to a modern Snowball Earth, Climate dynamics, 35, 887–905, 2010.

Voigt, A., Abbot, D. S., Pierrehumbert, R. T., and Marotzke, J.: Initiation of a Marinoan Snow ball Earth in a state-of-the-art atmosphere-ocean general circulation model, Climate of the Past, 7, 249–263, 2011.

Wagner, T. J. and Eisenman, I.: How Climate Model Complexity Influences Sea Ice Stability, Journal of Climate, 28, 3998–4014, 2015.

Weertman, J.: Deformation of floating ice shelves, Journal of Glaciology, 3, 38–42, 1957.

Yang, J., Peltier, W. R., and Hu, Y.: The Initiation of Modern'Soft Snowball'and'Hard Snowball'Climates in CCSM3. Part I: The Influences of Solar Luminosity, CO 2 Concentration, and the Sea Ice/Snow Albedo Parameterization., Journal of Climate, 25, 2012a.

Yang, J., Peltier, W. R., and Hu, Y.: The Initiation of Modern'Soft Snowball'and'Hard Snowball'Climates in CCSM3. Part II: Climate Dynamic Feedbacks., Journal of Climate, 25, 2012b.

Table 1. Summary of results. Asterisk indicates simulations with insolation at 94% of present day values. Negative circulation values indicate surface poleward flow.

Simulation	Emissivity	Circ.	Heat Transport
ice free	~~$\varepsilon = 0.6$~~ $\varepsilon = 0.5$	~~-28.8~~ -62.18 Sv	~~8.1e-1~~ 3.73 PW
partial ice	$\varepsilon = 0.7$	~~-26.6~~ -44.44 Sv	~~6.7e-1~~ 1.83 PW
near global ice*	~~$\varepsilon = 0.84$~~ $\varepsilon = 0.82$	~~2.7~~ -16.46 Sv	~~1.9e-3~~ 6.27e-4 PW
global ice*	~~$\varepsilon = 0.85$~~ $\varepsilon = 0.83$	~~4.9~~ -17.46 Sv	~~3.3e-4~~ 3.34e-2 PW

Table 2. Physical parameters used in simulations. See text for details on model initialization and settings of unconstrained parameters.

Parameter	Symbol	Units	Value
hemispheric extent	ℓ	θ	$\pi/2$
extent of Box 2 and 3	ζ	θ	$\pi/4$
depth of Box 1 and 2	d_u	m	200
depth of Box 3 and 4	d_l	m	3000
volume of Box 1	V_{ut}	m^3	2.83×10^{16}
volume of Box 2	V_{up}	m^3	1.17×10^{16}
volume of Box 3	V_{dp}	m^3	1.76×10^{17}
volume of Box 4	V_{dt}	m^3	4.25×10^{17}
Earth's radius	r_E	m	6.371×10^7
hydraulic constant	k_0	$\mathrm{m}^6 \cdot \mathrm{kg}^{-1} \cdot \mathrm{s}^{-1}$	7.8×10^7
reference density	ρ_0	$\mathrm{kg} \cdot \mathrm{m}^{-3}$	1027
reference salinity	S_0	psu	35
reference temperature	T_0	K	283
salinity exp. coefficient	β_S	psu^{-1}	7.61×10^{-4}
temperature exp. coefficient	β_T	K^{-1}	1.668×10^{-4}
ocean albedo	α_w	-	0.32
sea ice albedo	α_i	-	0.62
ocean water heat capacity	c_w	$\mathrm{J} \cdot \mathrm{kg}^{-1} \cdot \mathrm{K}^{-1}$	3996
sea ice heat capacity	c_i	$\mathrm{J} \cdot \mathrm{kg}^{-1} \cdot \mathrm{K}^{-1}$	2100
ocean water density	ρ_w	$\mathrm{kg} \cdot \mathrm{m}^{-3}$	1027
ice density	ρ_i	$\mathrm{kg} \cdot \mathrm{m}^{-3}$	917
ocean water conductivity	κ_w	$\mathrm{W} \cdot \mathrm{m}^{-1} \cdot \mathrm{K}^{-1}$	0.575
sea ice conductivity	κ_i	$\mathrm{W} \cdot \mathrm{m}^{-1} \cdot \mathrm{K}^{-1}$	2.5
sea ice latent heat	L	$\mathrm{J} \cdot \mathrm{kg}^{-1}$	3.34×10^5
freezing temperature	T_f	K	271.2
Stefan-Boltzmann constant	σ	$\mathrm{J} \cdot \mathrm{m}^{-2} \cdot \mathrm{s} \cdot \mathrm{K}^{-4}$	5.6704×10^{-8}
ice/ocean boundary layer	D	m	0.05
ice viscosity parameter	A_0	$\mathrm{Pa}^{-3}\mathrm{s}^{-1}$	$3.61 \cdot 10^{-13}$ $T < 263.15$; $1.734 \cdot 10^3$ $T > 263.15$.
ice viscosity parameter	Q	$\mathrm{J} \cdot \mathrm{mol}^{-1}$	$60 \cdot 10^3$ $T < 263.15$; $139 \cdot 10^3$ $T > 263.15$.
gas constant	R	$\mathrm{J} \cdot \mathrm{K}^{-1} \cdot \mathrm{mol}^{-1}$	8.31446
acceleration due to gravity	g	$\mathrm{m} \cdot \mathrm{s}^{-2}$	9.8
Glen's flow law exponent	n	-	3
geothermal heat forcing	F_g	$\mathrm{W} \cdot \mathrm{m}^{-2}$	0.05